

## Structure and surface kinetics of bismuth adsorption on Si(001)

Yonglin Qian and Michael J. Bedzyk\*

*Materials Science Division, Argonne National Laboratory, Argonne, Illinois 60439  
and Department of Materials Science and Engineering, Northwestern University, Evanston, Illinois 60208*

Paul F. Lyman and Tien-Lin Lee

*Materials Research Center, Northwestern University, Evanston, Illinois 60208  
and Department of Materials Science and Engineering, Northwestern University, Evanston, Illinois 60208*

Shaoping Tang<sup>†</sup> and A. J. Freeman

*Materials Research Center, Northwestern University, Evanston, Illinois 60208  
and Department of Physics and Astronomy, Northwestern University, Evanston, Illinois 60208*

(Received 29 February 1996)

X-ray standing wave measurements, along with local-density molecular cluster calculations, were used to determine the surface structure of the low-coverage Bi/Si(001) surface. The  $2 \times 2$  Bi phase, predicted by theory to be the stable low-coverage structure, was found experimentally to be a metastable phase and was observed to have a thermally activated irreversible phase transition to the stable  $1 \times 2$  phase. These measurements represent another approach for investigating the kinetics of surface reactions. [S0163-1829(96)04532-8]

An accurate description of kinetic processes on crystalline surfaces at the atomic scale is important for understanding thin-film growth, catalysis, and corrosion. For a detailed picture of adsorption, diffusion, nucleation, and bonding, a structural probe with both high resolution and chemical sensitivity is needed. By exploiting these traits, the x-ray standing-wave (XSW) method can be used to effectively complement more traditional probes of surface kinetics, such as scanning tunneling microscopy<sup>1</sup> (STM) and diffraction-based techniques [including low-energy electron diffraction (LEED) and surface x-ray diffraction]. As a probe of short-range order, the XSW method is complementary to diffraction and can be used to monitor transitions between adsorbate phases lacking long-range order. The XSW method is complementary to STM since it naturally provides statistical averaging over macroscopic areas; moreover, it is free from tip-surface interactions that can alter the kinetics of observed processes. Here we present an XSW study of the transformation kinetics between two structures found in the adsorption of Bi on Si(001); we thereby demonstrate how the XSW method can be used to advantage in cases not amenable to analysis by other techniques.

The adsorption of group-V elements on Si(001) has garnered much attention for its technological importance in heteroepitaxy, surface passivation,  $\delta$ -doping, and surfactant-mediated epitaxy.<sup>2-4</sup> Also, fundamental interest arises from the simple surface termination that often results.<sup>5-8</sup> Bismuth, the heaviest group-V element, has attracted particular interest since a recent STM and LEED study<sup>9</sup> of Bi adsorption on Si(001) at room temperature (RT) observed two distinct local structures: one with a  $2 \times 2$  periodicity for a Bi coverage below 0.5 ML (where 1 ML =  $6.78 \times 10^{14}$  atoms/cm<sup>2</sup>) and the other with a  $1 \times 2$  structure above 0.5 ML. Coverage-dependent surface structures had never been reported for other group-V elements (As and Sb). Using first-principles local-density molecular cluster calculations, Tang and Free-

man proposed that there are two stable phases for the Bi/Si(001) surface.<sup>10</sup> (Fig. 1). The theory predicts that a  $2 \times 2$  phase occurs at low coverage (below 0.5 ML) where Bi forms dimers on top of the Si dimerized surface. At higher coverages, the theory predicts that the  $2 \times 1$  reconstruction is removed and a  $1 \times 2$  Bi phase forms (just as for As or Sb adsorption). In previous XSW studies,<sup>11,12</sup> the structure of the  $1 \times 2$  Bi phase was precisely measured; the Bi dimer height and bond length agreed with the predicted values.<sup>10,11</sup> However, no quantitative experimental information has been reported for the  $2 \times 2$  phase.

Herein, we report XSW and cluster calculation results that seek to quantify the structure of the Bi/Si(001)-( $2 \times 2$ ) phase and the surface reaction kinetics for the thermally activated

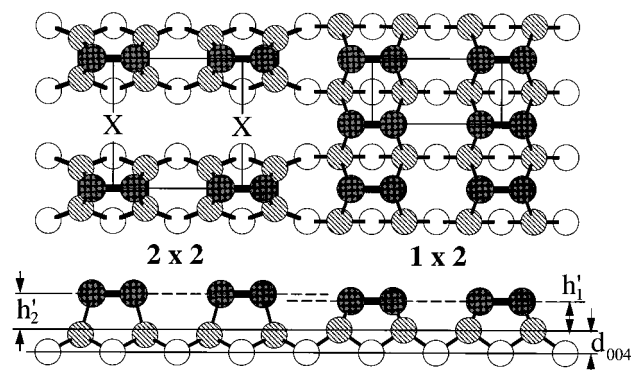


FIG. 1. Top view and side view of the  $2 \times 2$  (left-hand side) and  $1 \times 2$  (right-hand side) Bi phases on the Si(001) surface proposed by Tang and Freeman (Ref. 10). The open circles are bulk Si atoms, the hatched circles are top-layer Si atoms, and the dark circles are Bi atoms.  $h_1'$  and  $h_2'$  are the respective heights of the  $1 \times 2$  and  $2 \times 2$  phase Bi dimers above the Si(004) bulk-extrapolated lattice plane. The topmost (004) lattice planes are depicted as a pair of parallel lines.

transition between the  $2 \times 2$  and  $1 \times 2$  phases. The XSW method is ideally suited for studying such a reaction as it is extremely sensitive to the distinct heights of the Bi dimers depicted in Fig. 1.

The present theoretical calculations were performed using a first-principles local-density molecular cluster total-energy approach (DMol, Ref. 13). In a previous study<sup>11</sup> of the  $1 \times 2$  Bi phase, we calculated that Bi dimers are adsorbed at a height of  $h'_1 = 1.80 \text{ \AA}$  above the Si(001)- $1 \times 1$  surface and the Bi dimer bond length is  $L = 3.16 \text{ \AA}$ . These calculations are in reasonable agreement with the XSW experimental results<sup>11</sup> of  $h'_1 = 1.73 \pm 0.01 \text{ \AA}$  and  $L = 2.94 \pm 0.06 \text{ \AA}$ . In our present study, we focus on the  $2 \times 2$  Bi phase, in which the Bi dimer is predicted<sup>10</sup> to adsorb on the Si dimerized surface without breaking the Si dimers. A 33-atom cluster model<sup>14</sup> was used in this calculation. The Bi dimer bond length was calculated to be  $3.14 \text{ \AA}$ . The calculations also show that the Bi dimer is adsorbed at a height  $2.49 \text{ \AA}$  above the dimerized Si surface layer. With the Si dimers relaxed inward by  $0.37 \text{ \AA}$  relative to the unrelaxed Si(001)-( $1 \times 1$ ) surface, the height of the Bi dimer above the unrelaxed surface is therefore  $h'_2 = 2.12 \text{ \AA}$ . The height of the Bi dimer is clearly different for the  $1 \times 2$  and  $2 \times 2$  Bi phases and should therefore be very distinguishable by (004) XSW measurements.

Experimentally, we deposited 0.2 ML of Bi on Si(001) at RT and observed two ordered phases of Bi coexisting at the surface, as well as a “disordered” Bi component (i.e., Bi with a random distribution when projected onto the  $c$  axis of the Si substrate unit cell). The subsequent isochronal annealing study clearly indicated that the  $2 \times 2$  ordered phase and the disordered (or uncorrelated) Bi undergo a thermally activated irreversible transition to the stable ( $1 \times 2$ ) Bi phase.

For single-crystal Bragg diffraction, an XSW results from the interference of the incident and Bragg-reflected x-ray plane waves in and above the crystal with a period equal to the  $d$  spacing of the diffraction planes. As the incident angle  $\theta$  is scanned through the rocking curve of the Bragg reflection, the nodes and antinodes of the XSW move inward by one-half of a  $d$  spacing due to a  $\pi$ -rad phase shift of the reflected plane wave. This inward sweep of the XSW induces a characteristic modulation in the surface adatoms' fluorescence yield whose angular dependence can be described as

$$Y(\theta) = Y_{\text{OB}} \{1 + R + 2\sqrt{R}f_H \cos[v - 2\pi P_H]\}, \quad (1)$$

where the off-Bragg yield  $Y_{\text{OB}}$  is proportional to the adatom coverage and the reflectivity  $R(\theta)$  and the phase  $v(\theta)$  of the reflected plane wave are derived from x-ray dynamical diffraction theory. Model-independent parameters  $f_H$  and  $P_H$  (coherent fraction and coherent position) are the amplitude and phase of the  $H$ th Fourier component of the time-averaged spatial distribution of the adatoms. The coherent position is the  $\Delta d/d$  average position. By the convolution theorem, the coherent fraction can be written as  $f_H = Ca_H D_H$ , where the ordered fraction  $C$  is the fraction of adatoms at ordered positions, the geometrical factor  $a_H$  reflects the spatial arrangement of these ordered positions projected into a unit cell, and the Debye-Waller factor  $D_H$  accounts for thermal vibration of the adatoms.<sup>15</sup>

The experiment was conducted at beam line X15A of the National Synchrotron Light Source at Brookhaven National

Laboratory. The UHV system at X15A comprises four connected chambers for sample introduction, preparation, characterization, and x-ray measurements.<sup>16</sup> The Si(001) sample was Syton polished and Shiraki etched before introduction into the UHV system. The sample was heated to 1170 K for 10 min to desorb the protective oxide layer. After cooling to RT, LEED revealed a sharp, two-domain ( $2 \times 1$ ) pattern. Carbon and oxygen contamination were less than 0.02 ML by Auger electron spectroscopy (AES). 0.2 ML of Bi was then evaporated from a Knudsen cell (670 K) onto the RT Si surface. For Bi at 670 K, the vapor phase consists of both dimers and monomers.<sup>17</sup> The Bi coverage was calibrated by a quartz-oscillator thickness monitor and by the Bi AES peak ratio relative to the saturated coverage ( $\sim 0.8 \text{ ML}$ ).<sup>11,18</sup> The LEED pattern was still two domain ( $2 \times 1$ ) after deposition but fainter than that of the clean surface. The absence of a  $2 \times 2$  LEED pattern is consistent, however, with the small domain size observed by STM.<sup>9</sup>

An XSW measurement using the Si(004) reflection was then performed at an incident photon energy of  $E_\gamma = 13.7 \text{ keV}$  by scanning the incident energy through the (004) rocking curve. (For convenience, we convert the energy scale into a relative angle scale by Bragg's law.) At each angular step, the reflected x-ray intensity  $R$  and Bi  $L\alpha$  fluorescence yield were recorded. After the “as-deposited” XSW measurement, the sample was annealed for 20 min at successively higher temperatures and cooled down to RT for subsequent XSW measurements. The XSW data collection time was 2 h for each anneal. The entire experiment lasted 24 h. Bi desorption started above 720 K. Figure 2 illustrates the angular dependence of the Si(004) reflectivity, Bi  $L\alpha$  fluorescence yields (circles), and the best fit to the dynamical diffraction theory<sup>19</sup> (smooth curves). The modulations in the Bi fluorescence yields are due to the inward phase shift of the XSW relative to the (004) diffraction planes. Two important features are evident in the data by inspection. First, the Bi modulation amplitude (or coherent fraction) shows a substantial increase with annealing temperature, indicating that the Bi atom population is tending towards a single adsorption height. Second, the position of the maximum in the Bi yield curve moves to larger angles as the surface is annealed to higher temperatures, indicating that the average Bi position is moving inward. This is a signature of a transition from the  $2 \times 2$  phase to  $1 \times 2$  phase. (See Fig. 1.) In a previous XSW study<sup>20</sup> of the Au/Si(111) surface, a similar sensitivity was seen to the process of annealing.

From the best fit of Eq. (1) to the data in Fig. 2, we determined the coherent fraction  $f_{004}$ , the coherent position  $P_{004}$ , and the off-Bragg fluorescence yield  $Y_{\text{OB}}$ . (The tabular inset in Fig. 2 lists the  $f_{004}$  and  $P_{004}$  values.) At the high temperature end, we measured a high coherent fraction of 0.75 and a coherent position of 1.29. Thus the surface is highly ordered after annealing to 720 K. That the coherent position approaches the value of 1.27 found for the  $1 \times 2$  phase by previous XSW measurements<sup>11,12</sup> indicates that the surface is approaching the stable  $1 \times 2$  phase after annealing. At low annealing temperatures, the coherent fraction is low (0.3) and the coherent position (1.50) differs greatly from that of the  $1 \times 2$  phase. This indicates the existence of another ordered phase, namely, the  $2 \times 2$  phase. The coexistence of the  $2 \times 2$  and  $1 \times 2$  phases is evidenced by two ob-

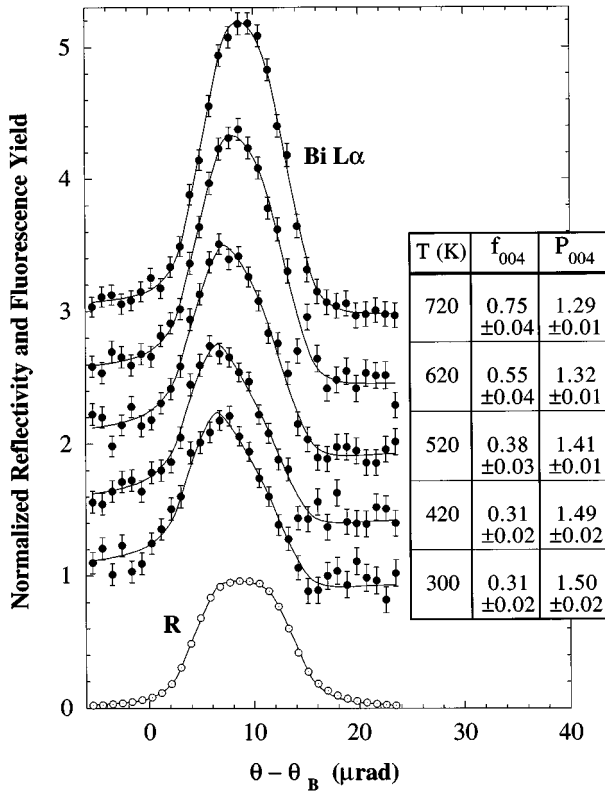


FIG. 2. Series of experimental data (dots) and best fits to x-ray dynamical diffraction theory (solid lines) for the Si(004) reflectivity and normalized Bi  $L\alpha$  fluorescence yield as a function of incident angle  $\theta$  for RT measurements after various annealing temperatures  $T$ . The curves at increasing  $T$  are offset for clarity. The values of  $T$ ,  $f_{004}$  and  $P_{004}$  are listed in the tabular inset.

servables. First, the measured coherent position (1.50) does not quite reach the  $2 \times 2$  theoretical value of  $2.12 \text{ \AA} / d_{004} = 1.55$ , but falls between this value and that of the  $1 \times 2$  phase. The second indication is the rather low coherent fraction, which is partially attributable to the two Bi adsorption heights reducing the geometrical factor  $a_{004}$ . Disordered (or uncorrelated) Bi, present at low annealing temperatures, also reduces the coherent fraction.

Based on our experimental results and theoretical calculations, we can determine the compositions of the two ordered phases as well as the disordered Bi. The adsorption heights of the symmetric Bi ad-dimers relative to the Si(004) bulk-extrapolated surface are  $h'_1$  for the  $1 \times 2$  phase and  $h'_2$  for the  $2 \times 2$  phase (Fig. 1). If the compositions of these two ordered Bi phases are denoted  $C_{1 \times 2}$  and  $C_{2 \times 2}$ , the resultant (004) Fourier component for the Bi adatoms' spatial distribution is

$$f_{004} \exp(2\pi i P_{004}) = D_{004} [C_{1 \times 2} \exp(2\pi i P_1) + C_{2 \times 2} \exp(2\pi i P_2)], \quad (2)$$

where  $P_1 = h'_1 / d_{004}$  and  $P_2 = h'_2 / d_{004}$  are the Bi fractional positions relative to the Si(004) diffraction planes and  $f_{004}$  and  $P_{004}$  are the experimental observables. For the  $1 \times 2$  phase, prior XSW measurements<sup>11,12</sup> determined  $P_1$  to be 1.27. For the  $2 \times 2$  phase, we employ the theoretical value of

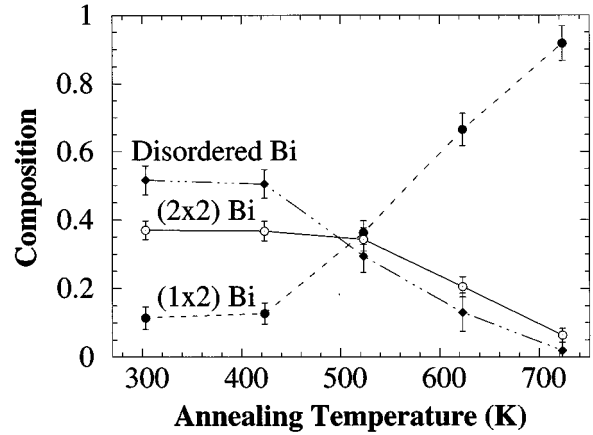


FIG. 3. Derived phase compositions of Bi as a function of annealing temperature. The lines are drawn to guide the eye.

$P_2 = 1.55$  since no direct measurement of the  $2 \times 2$  Bi dimer height exists. For the RT Debye-Waller factor, we use  $D_{004} = 0.83 \pm 0.03$  from a separate XSW study<sup>12</sup> of the  $1 \times 2$  phase that measured both the (004) and (008) Fourier components. This corresponds to a Bi vibrational amplitude of  $\sqrt{\langle u_{001}^2 \rangle} = 0.13 \pm 0.015 \text{ \AA}$ , which is also consistent with the XSW-measured thermal vibration amplitudes for As (Ref. 5) and Sb (Ref. 21) ad-dimers on Si(001). The determined compositions of the three phases are plotted in Fig. 3 as a function of the annealing temperature.

Below 420 K, the Bi distribution did not change. After annealing to 520 K, 50% of the disordered Bi and 10% of the  $2 \times 2$  phase were converted into the  $1 \times 2$  phase. The conversion of the disordered Bi started between 420 and 520 K, while the conversion of the  $2 \times 2$  phase started at about 520 K. Clearly, even at this low coverage of 0.2 ML, the  $2 \times 2$  phase is not stable as predicted,<sup>10</sup> but is instead a metastable phase. For temperatures up to 720 K, the off-Bragg Bi fluorescence yield  $Y_{OB}$  remained constant, indicating that no Bi desorbed.

From the data acquired after each annealing interval, we can determine the reduction in the  $2 \times 2$  phase population during the interval. To determine a conversion rate  $\lambda$  for each temperature, we describe the  $2 \times 2$  population during each short annealing interval as  $N(t) = N_0 e^{-\lambda t}$ . In Fig. 4 we plot these experimentally determined values of  $\lambda$  versus in-

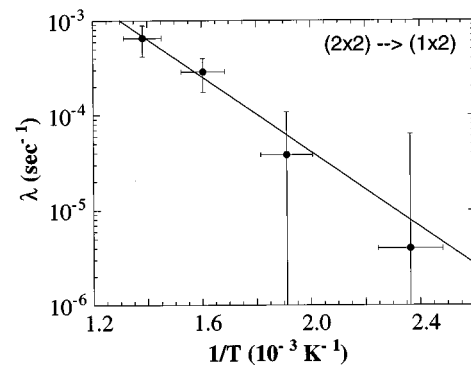


FIG. 4. Conversion rate of the  $2 \times 2$  Bi phase to the  $1 \times 2$  as a function of annealing temperature.

verse temperature  $1/T$ . The correspondence of the data to the Arrhenius form suggests describing the conversion as thermally activated, with a conversion rate given by  $\lambda = \lambda_0 e^{-E_A/kT}$ . From the fit (solid line in Fig. 4), we find an effective activation energy of  $E_A = 0.4 \pm 0.2$  eV, with an exponential prefactor (effective attempt frequency) of  $\lambda_0 \sim 10^{-1}$  Hz.

Let us consider a mechanism for the metastable-to-stable phase transition of  $2 \times 2$  to  $1 \times 2$ . Similar to the cluster calculation for a reduced Bi/Si(001) surface model,<sup>10</sup> introducing an extra Bi atom (or dimer) to a vacancy site (indicated by  $X$  in Fig. 1) between the  $2 \times 2$  phase Bi dimers would break the neighboring Si dimers. This configuration serves as a precursor state leading to a Bi  $1 \times 2$  phase and can be achieved either by adsorbing more Bi from the gas phase onto the surface, as accounted for in the cluster calculations,<sup>10</sup> or by annealing the surface to give existing Bi atoms sufficient mobility to achieve a thermally activated phase transition, as was done in our experiment. We infer, then, that for a low-coverage surface annealed to modest temperatures, the mobility of Bi atoms is low, precluding the Bi migration required to form the precursor configuration. This accounts for the low observed exponential prefactor and explains why the  $2 \times 2$  phase persisted to 520 K despite the

low-energy barrier (0.4 eV). Due to the statistical averaging inherent in the XSW method, we can establish the energy scale for these important atomic scale phenomena directly and noninvasively, without needing to know or examine all possible reaction pathways.

We can compare our experimental results to those of a recent STM study of the thermal conversion of  $Sb_4$  precursors on Si(001) to their final adsorption state.<sup>22</sup> Our measured activation energy is close to the value (0.5 eV) measured for  $Sb_4$  precursors. However, the prefactor for the Bi  $2 \times 2$  to  $1 \times 2$  conversion is four orders of magnitude lower than that for  $Sb_4$  precursors. One important difference in their studies is the fact that Sb evaporates as quaterners, whereas Bi evaporates chiefly as monomers and dimers. Hence a pair of neighboring Sb dimers can be formed without mass transport. The considerably lower exponential prefactor found in our study very likely reflects the diffusion required to create stable pairs of Bi  $1 \times 2$  dimers.

This work was sponsored by the DOE under Contracts Nos. W-31-109-ENG-38 to Argonne National Laboratory and DE-AC02-76CH00016 to the National Synchrotron Light Source and by the NSF under Contract No. DMR-9120521 to the MRC at Northwestern University.

\* Author to whom correspondence should be addressed.

<sup>†</sup> Present address: Materials Science Laboratory, Texas Instruments, Inc., Dallas, TX 75243.

<sup>1</sup> For a review, see M. G. Lagally, *Jpn. J. Appl. Phys.* **32**, 1493 (1993).

<sup>2</sup> R. D. Bringans, R. I. G. Uhrberg, M. A. Olmstead, and R. Z. Bachrach, *Phys. Rev. B* **34**, 7447 (1986).

<sup>3</sup> R. D. Bringans, D. K. Biegelsen, J. E. Northrup, and L.-E. Swartz, *Jpn. J. Appl. Phys.* **32**, 1484 (1993).

<sup>4</sup> M. Copel, M. C. Reuter, E. Kaxiras, and R. M. Tromp, *Phys. Rev. Lett.* **63**, 632 (1989); M. Horn-von Hoegen, F. K. LeGoues, M. Copel, M. C. Reuter, and R. M. Tromp, *ibid.* **67**, 1130 (1991); K. Sakamoto, K. Kyoya, K. Miki, and T. Hashizume, *Jpn. J. Appl. Phys.* **32**, L204 (1993).

<sup>5</sup> G. E. Franklin, E. Fontes, Y. Qian, M. J. Bedzyk, J. A. Golovchenko, and J. R. Patel, *Phys. Rev. B* **50**, 7483 (1994).

<sup>6</sup> S. Tang and A. J. Freeman, *Phys. Rev. B* **47**, 1460 (1993); **48**, 8086 (1993).

<sup>7</sup> M. Richter *et al.* *Phys. Rev. Lett.* **65**, 3417 (1990).

<sup>8</sup> P. F. Lyman, Y. Qian, and M. J. Bedzyk, *Surf. Sci.* **325**, L385 (1995).

<sup>9</sup> H. P. Noh *et al.*, *J. Vac. Sci. Technol. B* **12**, 2097 (1994).

<sup>10</sup> S. Tang and A. J. Freeman, *Phys. Rev. B* **50**, 1701 (1994).

<sup>11</sup> G. E. Franklin, S. Tang, J. C. Woicik, M. J. Bedzyk, A. J. Freeman, and J. A. Golovchenko, *Phys. Rev. B* **52**, R5515 (1995).

<sup>12</sup> P. F. Lyman, Y. Qian, T.-L. Lee, and M. J. Bedzyk, *Physica B* **221**, 426 (1996).

<sup>13</sup> B. Delley, *J. Chem. Phys.* **92**, 508 (1990); **94**, 7245 (1991).

<sup>14</sup> See Fig. 3(b) in S. Tang, A. J. Freeman, Y. Qian, G. E. Franklin, and M. J. Bedzyk, *Phys. Rev. B* **51**, 1593 (1995).

<sup>15</sup> M. J. Bedzyk and G. Materlik, *Phys. Rev. B* **31**, 4110 (1985).

<sup>16</sup> J. Zegenhagen, *Surf. Sci. Rep.* **18**, 199 (1993).

<sup>17</sup> A. Kawazu, T. Otsuki, and G. Tominaga, *Jpn. J. Appl. Phys.* **20**, 553 (1981).

<sup>18</sup> C. Park, R. Z. Bakhtizin, T. Hashizume, and T. Sakurai, *Jpn. J. Appl. Phys.* **32**, L528 (1993).

<sup>19</sup> For a review, see B. W. Batterman and H. Cole, *Rev. Mod. Phys.* **36**, 681 (1964).

<sup>20</sup> S. M. Durbin, L. E. Berman, B. W. Batterman, and J. M. Blakely, *Phys. Rev. B* **33**, 4402 (1986); L. E. Berman, B. W. Batterman, and J. M. Blakely, *ibid.* **38**, 5397 (1988).

<sup>21</sup> Y. Qian, P. F. Lyman, T.-L. Lee, and M. J. Bedzyk, *Physica B* **221**, 430 (1996).

<sup>22</sup> Y. W. Mo, *Phys. Rev. Lett.* **69**, 3643 (1992).